

# An Empirical Exploration of Cross-domain Alignment between Language and Electroencephalogram

William Han<sup>1\*</sup>, Jielin Qiu<sup>1\*</sup>, Jiacheng Zhu<sup>1</sup>, Mengdi Xu<sup>1</sup>, Douglas Weber<sup>1</sup>, Bo Li<sup>2</sup>, Ding Zhao<sup>1</sup>

<sup>1</sup> Carnegie Mellon University <sup>2</sup> University of Illinois Urbana-Champaign

## Abstract

Electroencephalography (EEG) and language have been widely explored independently for many downstream tasks (e.g., sentiment analysis, relation detection, etc.). Multimodal approaches that study both domains have not been well explored, even though in recent years, multimodal learning has been seen to be more powerful than its unimodal counterparts. In this study, we want to explore the relationship and dependency between EEG and language, i.e., how one domain reflects and represents the other. To study the relationship at the representation level, we introduced **MTAM**, a **M**ultimodal **T**ransformer **A**lignment **M**odel, to observe coordinated representations between the two modalities, and thus employ the transformed representations for downstream applications. We used various relationship alignment-seeking techniques, such as Canonical Correlation Analysis and Wasserstein Distance, as loss functions to transfigure low-level language and EEG features to high-level transformed features. On downstream applications, sentiment analysis and relation detection, we achieved new state-of-the-art results on two datasets, ZuCo and K-EmoCon. Our method achieved an F1-score improvement of 16.5% on sentiment analysis for K-EmoCon, 27% on sentiment analysis of ZuCo, and 31.1% on relation detection of ZuCo. In addition, we provide interpretations of the performance improvement by: (1) visualizing the original feature distribution and the transformed feature distribution, showing the effectiveness of the alignment module for discovering and encoding the relationship between EEG and language; (2) visualizing word-level and sentence-level EEG-language alignment weights, showing the influence of different language semantics as well as EEG frequency features; and (3) visualizing brain topographical maps to provide an intuitive demonstration of the connectivity of EEG and language response in the brain regions.

## Introduction

Brain activity is an important parameter in furthering our knowledge of how human language is represented and interpreted (Murphy, Wehbe, and Fyshe 2018; Toneva, Mitchell, and Wehbe 2020; Williams and Wehbe 2021; Reddy and Wehbe 2021; Wehbe et al. 2020; Deniz et al. 2021; Schwartz, Toneva, and Wehbe 2019). Researchers from domains such as linguistics, psychology, cognitive science, and

computer science have made large efforts in using brain-recording technologies to analyze cognitive activity during language related tasks and observed that these technologies have added value in terms of understanding language (Stemmer and Connolly 2012).

Basic linguistic rules seem to be effortlessly understood by humans in contrast to machinery. Recent advances in natural language processing (NLP) models (Vaswani et al. 2017) have enabled computers to maintain long and contextual information through self-attention mechanisms. This attention mechanism has been maneuvered to create robust language models but at the cost of tremendous amounts of data (Devlin et al. 2019; Liu et al. 2019b; Lewis et al. 2020; Brown et al. 2020; Yang et al. 2019). Although performance has significantly improved by using modern NLP models, they are still seen to be suboptimal compared to the human brain. Bisk et al. (2020) argues that the language-only approach in training reaches a point of diminishing returns and extra-linguistic factors are needed in comprehending language through computational procedures.

To combat the limitations of unimodal approaches in NLP, Linzen (2020) encouraged scholars for the gathering of multimodal data to accelerate comprehension and generalization of natural language in machinery. A popular multimodal framework encodes features from different modalities into a common latent space and maps the latent representations to a specified task (Huang et al. 2021). Huang et al. (2021) proves that learning with multiple modalities attains a smaller population risk and an accurate estimate of latent space representations. Most existing work in multimodal learning combines a variation of language, vision, and speech signals to perform a wide range of tasks, including but not limited to automatic image and video tagging, speech recognition, and identity classification (Elliott, Kiela, and Lazaridou 2016; Deng 2016; Yang et al. 2022; Kiros, Salakhutdinov, and Zemel 2014). More recently, physiological signals have gained attention in the NLP multimodal realm due to their abundance in information and proven practicality across many assignments (Hollenstein et al. 2019). In the context of modeling human-like learning phenomena for language, it is instinctively appealing to leverage physiological signals. However, in practice, wielding multiple modalities, including physiological signals and language, is often challenging due to the heterogeneity and

\*Equal contribution

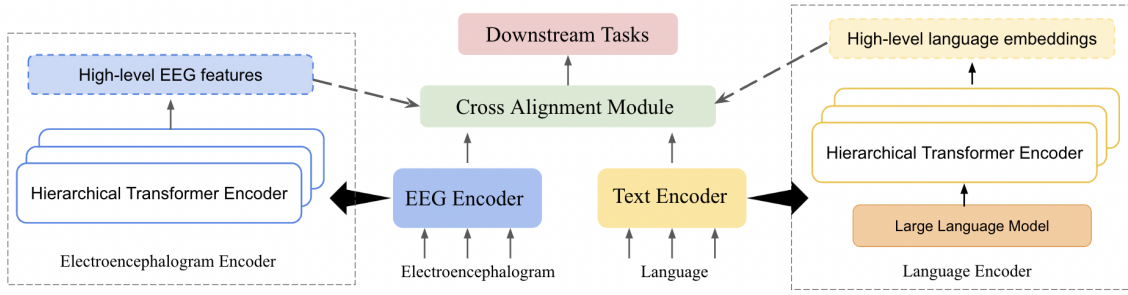


Figure 1: The architecture of our model, where EEG and language features are coordinately explored by two encoders. The EEG encoder and language encoder are shown on the left and right, respectively. The cross alignment module is used to explore the connectivity and relationship within two domains, while the transformed features are used for downstream tasks.

contingencies found in the data (Morency and Baltrusaitis 2017). Wang and Ji (2021) proposed a method for EEG-To-Text sequence-to-sequence decoding and achieved great performance, however, the real relationship and connectivity between EEG and language are not well studied.

In this study, we explore the relationship and dependencies of EEG and language. We apply EEG, a popularized routine in cognitive research for its accessibility and practicality, along with language to discover the connectivity.

Our contributions are summarized as follows:

- To the best of our knowledge, we are the first to explore the fundamental relationship and connectivity between EEG and language through computational multimodal alignment methods.
- We introduced **MTAM**, a **Multimodal Transformer Alignment Model**, that learns coordinated representations by hierarchical transformer encoders. The transformed representations showed tremendous performance improvements and state-of-the-art results in downstream applications, i.e., sentiment analysis and relation detection, on two datasets, ZuCo 1.0/2.0 and K-EmoCon.
- We carried out experiments with multiple alignment mechanisms, i.e., canonical correlation analysis and Wasserstein distance, and proved that relation-seeking loss functions are helpful in downstream tasks.
- We provided interpretations of the performance improvement by visualizing the original feature distribution and the transformed feature distribution, showing the effectiveness of the alignment module for discovering and encoding the relationship between EEG and language.
- Our findings on word-level and sentence-level EEG-language alignment showed the influence of different language semantics as well as EEG frequency features, which provided additional explanations.
- The brain topographical maps delivered an intuitive demonstration of the connectivity of EEG and language response in the brain regions, which issues a physiological basis of our discovery.

## Related Work

**Multimodal Learning** Formalized multimodal learning research dates back to 1989, when Yuh, Goldstein, and

Sejnowski (1989) conducted an experiment that built off the McGurk Effect for audio-visual speech recognition using neural networks (Tiippana 2014; McGurk and MacDonald 1976). Researchers in NLP and computer vision (CV) collaborated to make available large, multimodal datasets (Koelstra et al. 2012; Zheng and Lu 2015; Hollenstein et al. 2018; Park et al. 2020) catered towards specific downstream tasks, such as classification, translation, and detection.

### Multimodal Learning of EEG and Other Domains

EEG signal is a popular choice as a modality in multimodal learning. Ben Said et al. (2017) used EMG signals jointly with EEG in a bi-autoencoder architecture and increased accuracies for sentiment analysis. Bashar (2018) integrated ECG and EEG signals in a human identification task, where fused classifiers produced the highest score. Liu et al. (2019a, 2022); Bao et al. (2019) extracted correlated features between EEG and eye movement data for emotion classification, showing transformed features are more homogeneous and discriminative. Ortega and Faisal (2021) fed fNIRS and EEG to decode bimanual grip force and resulted in increased performance, comparing to single modality models. There are also efforts to find correlations between EEG and visual stimulus frequencies (Saeidi et al. 2021). A common theme occurring among these works showed EEG paired with other domains can boost performance.

### Multimodal Learning of Language and Other Brain Signals

Recently, language and cognitive data were also used together in multimodal settings to complete desirable tasks (Wang and Ji 2021; Hollenstein et al. 2019, 2021; Hollenstein, Barrett, and Beinborn 2020). Wehbe et al. (2014) used a recurrent neural network to perform word alignment between MEG activity and the generated word embeddings. Toneva and Wehbe (2019) utilized word-level MEG and fMRI recordings to compare word embeddings from large language models. Schwartz, Toneva, and Wehbe (2019) used MEG and fMRI data to fine-tune a BERT language model (Devlin et al. 2019) and found that the relationships between these two modalities were generalized across participants. Huang et al. (2020) leveraged CT images and text from electronic health records to classify pulmonary embolism cases and observed that the multimodal model with late fusion achieved the best performance. Murphy et al. (2022)

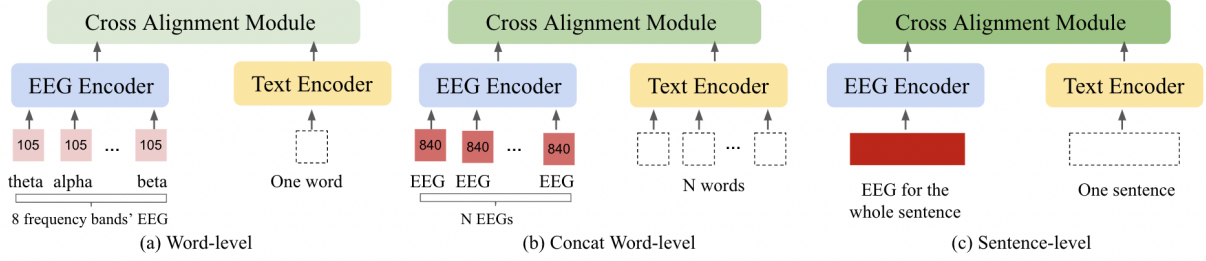


Figure 2: Three paradigms of EEG and language alignment.

used MEG and EEG signals to find semantic categories in language. However, the relationship between language and EEG has not been explored before.

**Multimodal Learning of EEG and Language** Hale et al. (2019) related EEG signals to the states of a neural phrase structure parser and showed that through EEG signals, models were correlating syntactic properties to a specific genre of text. Foster et al. (2021) applied EEG signals to predict specific values of each dimension in a word vector through regression models. Wang and Ji (2021) used word-level EEG features to decode corresponding text tokens through an open vocabulary, sequence-to-sequence framework. Hollenstein et al. (2021) focused on a multimodal approach by utilizing a combination of EEG, eye-tracking, and text data to improve NLP tasks. They used a variation of LSTM and CNN to decode the EEG features, but did not explore the relationship between EEG and language. Their proposed multimodal framework follows the bi-encoder approach (Choi et al. 2021) where the two modalities are encoded separately (Hollenstein et al. 2021).

## Methods

### Overview of Model Architecture

The architecture of our model is shown in Fig. 1. The bi-encoder architecture is helpful in projecting embeddings into vector space for methodical analysis (Liu et al. 2019a; Hollenstein et al. 2021; Choi et al. 2021). Thus in our study, we adopt the bi-encoder approach to effectively reveal hidden relations between language and EEG. The **MTAM**, Multimodal Transformer Alignment Model, contains several modules. We use a dual-encoder architecture, where each view contains hierarchical transformer encoders. The inputs of each encoder are EEG and language, respectively. For EEG hierarchical encoders, each encoder shares the same architecture as the encoder module in Vaswani et al. (2017). In the current literature, researchers assume that the brain acts as an encoder for high-dimensional semantic representations (Wang and Ji 2021; Gauthier and Ivanova 2018; Correia et al. 2013). Based on this assumption, the EEG signals act as low-level embeddings. By feeding it into its respective hierarchical encoder, we extract transformed EEG embeddings as input for the cross alignment module. As for the language path, the language encoder is slightly different from the EEG encoder. We first process the text with a

pretrained large language model (LLM) to extract text embeddings and then use hierarchical transformer encoders to transform the raw text embeddings into high-level features. The mechanism of the cross alignment module is to explore the inner relationship between EEG and language through a connectivity-based loss function. In our study, we investigate several alignment methods, i.e., Canonical Correlation Analysis (CCA) and Wasserstein Distance (WD). The output features from the cross alignment module can be used for downstream applications. The details of each part will be introduced in the following sections.

### Hierarchical Transformer Encoders

Let  $X_e \in \mathbb{R}^{D_e}$  and  $X_t \in \mathbb{R}^{D_t}$  be the two normalized input feature matrices for EEG and text, respectively, where  $D_e$  and  $D_t$  describes the dimensions of the feature matrices. To encode the two feature vectors, we feed them to their hierarchical transformer encoders:  $V_e = E_e(X_e; W_e)$ ;  $V_t = E_t(X_t; W_t)$ , where  $E_e$  and  $E_t$  denotes the separate encoders,  $V_e$  and  $V_t$  symbolizes the outputs for the transformed low-level features and  $W_e$  and  $W_t$  denotes the trainable weights for EEG and text respectively.

The outputs of these two encoders can be further expanded by stating  $V_e = [v_e^1, v_e^2, v_e^3, \dots, v_e^n] \in \mathbb{R}^n$  and  $V_t = [v_t^1, v_t^2, v_t^3, \dots, v_t^k] \in \mathbb{R}^k$ , where  $n$  and  $k$  denotes the number of instances in a given output vector and  $v_e^n$  and  $v_t^k$  denotes the instance itself. Due to page limit, more details of the transformer encoders can be found in the Appendix.

### Cross Alignment Module

As shown in Fig. 2, there are three paradigms of EEG and language alignment. For word level, the EEG features are divided by each word, and the objective of the alignment is to find the connectivity of different frequencies with the corresponding word. For the concat-word level, the 8 frequencies' EEG features are concatenated as a whole, and then concatenated again to match the corresponding sentence, so the alignment is to find out the relationship within the sentence. As for sentence-level, the EEG features are calculated as an average over the word-level EEG features. There is no boundary for the word, so the alignment module tries to encode the embeddings as a whole, and explore the general representations. In the Cross Alignment Module (CAM), we introduced a new loss function in addition to the original cross-entropy loss. The new loss is based on Canonical

Correlation Analysis (CCA) (Andrew et al. 2013) and Optimal Transport (Wasserstein Distance). As in Andrew et al. (2013), CCA aims to concurrently learn the parameters of two networks to maximize the correlation between them. Wasserstein Distance (WD), which originates from Optimal Transport (OT), has the ability to align embeddings from different domains to explore the relationship (Chen et al. 2020).

**Canonical Correlation Analysis** Canonical Correlation Analysis (CCA) is a method for exploring the relationships between two multivariate sets of variables. It learns the linear transformation of two vectors to maximize the correlation between them, which is used in many multimodal problems (Andrew et al. 2013; Qiu, Liu, and Lu 2018; Gong et al. 2013). In this work, we apply CCA to capture the cross-domain relationship. Let low-level transformed EEG features be  $V_e$  and low-level language features be  $L_t$ . We assume  $(V_e, V_t) \in \mathbb{R}^{n_1} \times \mathbb{R}^{n_2}$  has covariances  $(\Sigma_{11}, \Sigma_{22})$  and cross-covariance  $\Sigma_{12}$ . CCA finds pairs of linear projections of the two views,  $(w_1' V_e, w_2' V_t)$  that are maximally correlated:

$$\begin{aligned} (w_1^*, w_2^*) &= \operatorname{argmax}_{w_1, w_2} \operatorname{corr}(w_1' V_e, w_2' V_t) \\ &= \operatorname{argmax}_{w_1, w_2} \frac{w_1' \Sigma_{12} w_2}{\sqrt{w_1' \Sigma_{11} w_1 w_2' \Sigma_{22} w_2}} \end{aligned} \quad (1)$$

Since the objective is invariant to scaling of  $w_1$  and  $w_2$ , the projections are constrained to have unit variance:

$$(w_1^*, w_2^*) = \operatorname{argmax}_{w_1' \Sigma_{11} w_1 = w_2' \Sigma_{22} w_2 = 1} w_1' \Sigma_{12} w_2 \quad (2)$$

In our study, we modified the structure of Andrew et al. (2013) while honoring its duty by replacing the neural networks with Transformer encoders.  $w_1^*$  and  $w_2^*$  denote the high-level, transformed weights from the low-level text and EEG features, respectively.

**Wasserstein Distance** Wasserstein Distance (WD) is introduced in Optimal Transport (OT), which is a natural type of divergence for registration problems as it accounts for the underlying geometry of the space, and has been used for multimodal data matching and alignment tasks (Chen et al. 2020; Yuan et al. 2020; Lee et al. 2019; Demetci et al. 2020; Qiu et al. 2022; Zhu et al. 2022). In Euclidean settings, OT introduces WD  $\mathcal{W}(\mu, \nu)$ , which measures the minimum effort required to “displace” points across measures  $\mu$  and  $\nu$ , where  $\mu$  and  $\nu$  are values observed in the empirical distribution. In our setting, we compute the temporal-pairwise Wasserstein Distance on EEG features and language features, which are  $(\mu, \nu) = (V_e, V_t)$ . For simplicity without loss of generality, assume  $\mu \in P(\mathbb{X})$  and  $\nu \in P(\mathbb{Y})$  denote the two discrete distributions, formulated as  $\mu = \sum_{i=1}^n u_i \delta_{x_i}$  and  $\nu = \sum_{j=1}^m v_j \delta_{y_j}$ , with  $\delta_x$  as the Dirac function centered on  $x$ .  $\Pi(\mu, \nu)$  denotes all the joint distributions  $\gamma(x, y)$ , with marginals  $\mu(x)$  and  $\nu(y)$ . The weight vectors  $u = \{u_i\}_{i=1}^n \in \Delta_n$  and  $v = \{v_j\}_{j=1}^m \in \Delta_m$  belong to the  $n$ - and  $m$ -dimensional simplex, respectively. The WD between the two discrete distributions  $\mu$  and  $\nu$  is defined as:

$$\mathcal{WD}(\mu, \nu) = \inf_{\gamma \in \Pi(\mu, \nu)} \mathbb{E}_{(x, y) \sim \gamma} [c(x, y)] = \min_{T \in \Pi(u, v)} \sum_{i=1}^n \sum_{j=1}^m T_{ij} \cdot c(x_i, y_j) \quad (3)$$

where  $\Pi(u, v) = \{T \in \mathbb{R}_+^{n \times m} \mid T \mathbf{1}_m = u, T^\top \mathbf{1}_n = v\}$ ,  $\mathbf{1}_n$  denotes an  $n$ -dimensional all-one vector, and  $c(x_i, y_j)$  is the cost function evaluating the distance between  $x_i$  and  $y_j$ .

**Loss Objective** The loss objective for the CAM module can be formalized as:  $Loss = l_{CE} + \alpha_1 l_{CCA} + \alpha_2 l_{WD}$ , where  $\alpha_i \in \{0, 1\}$ ,  $i \in (1, 2)$  controls the weights of different parts of alignment-based loss objective.

## Experiments

### Downstream Tasks

In this study, we evaluate our method on two downstream tasks: Sentiment Analysis (SA) and Relation Detection (RD) of two datasets: K-EmoCon (Park et al. 2020) and ZuCo 1.0/2.0 Dataset (Hollenstein et al. 2018, 2020).

**Sentiment Analysis (SA)** Given a succession of word-level or sentence-level EEG features and their corresponding language, the task is to predict the sentiment label. The ZuCo 1.0 dataset consists of sentences from the Stanford Sentiment Treebank, which contains movie reviews and their corresponding sentiment label (i.e., positive, neutral, negative) (Socher et al. 2013). The K-EmoCon dataset categorizes emotion annotations as valence, arousal, happy, sad, nervous, and angry. For each emotion, the participant labeled the extent of the given emotion felt by following a Likert-scale paradigm. Arousal and valence are rated 1 to 5 (1: very low; 5: very high). Happy, sad, nervous, and angry emotions are rated 1 to 4, where 1 means very low and 4 means very high. The ratings are dominantly labeled as very low and neutral. Therefore to combat class imbalance, we collapse the labels to binary and ternary settings.

**Relation Detection (RD)** The goal of relation detection (also known as relation extraction or entity association) is to extract semantic relations between entities in a given text. For example, in the sentence, “June Huh won the 2022 Fields Medal.”, the relation *AWARD* connects the two entities “June Huh” and “Fields Medal” together. The ZuCo 1.0/2.0 datasets provide the ground truth labels and texts for this task. We use texts from the Wikipedia relation extraction dataset (Culotta, McCallum, and Betz 2006) that has 10 relation categories: award, control, education, employer, founder, job title, nationality, political affiliation, visited, and wife (Hollenstein et al. 2018, 2020).

### Datasets

**K-EmoCon Dataset** K-EmoCon (Park et al. 2020) is a multimodal dataset including videos, speech audio, accelerometer, and physiological signals during a naturalistic conversation. After the conversation, each participant watched a recording of themselves and annotated their own and partner’s emotions. Five external annotators were recruited to annotate both parties’ emotions, six emotions in total (Arousal, Valence, Happy, Sad, Angry, Nervous). The NeuroSky MindWave headset captured EEG signals from the left prefrontal lobe (FP1) at a sampling rate of 125 Hz in 8 frequency bands: delta (0.5–2.75Hz), theta (3.5–6.75Hz), low-alpha (7.5–9.25Hz), high-alpha (10–11.75Hz), low-beta (13–16.75Hz), high-beta (18–29.75Hz), low-gamma

Table 1: Comparison with baselines on Zuco dataset.

Task	Model	Sentence Level				Word Level				Concat Word Level			
		Prec	Rec	F1	Acc	Prec	Rec	F1	Acc	Prec	Rec	F1	Acc
Sentiment Analysis	MLP-EEG	0.644	0.637	0.640	0.666	0.602	0.644	0.622	0.630	0.597	0.618	0.607	0.600
	MLP-Text	0.359	0.357	0.357	0.373	0.380	0.388	0.384	0.387	0.210	0.243	0.225	0.228
	BiLSTM-EEG	0.675	0.656	0.664	0.666	0.677	0.659	0.668	0.671	0.612	0.609	0.610	0.608
	BiLSTM-Text	0.420	0.347	0.380	0.371	0.335	0.326	0.330	0.329	0.341	0.322	0.331	0.329
	Transformer-EEG	0.887	0.879	0.883	0.883	0.832	0.840	0.836	0.881	0.832	0.840	0.836	0.817
	Transformer-Text	0.548	0.546	0.547	0.507	0.527	0.533	0.530	0.582	0.558	0.547	0.552	0.550
	ResNet-EEG	0.687	0.678	0.682	0.683	0.707	0.718	0.712	0.709	0.691	0.689	0.690	0.688
	ResNet-Text	0.214	0.183	0.165	0.222	0.198	0.199	0.198	0.200	0.202	0.211	0.206	0.210
	RNN-Multimodal (Hollenstein et al. 2021)	—	—	—	—	0.728	0.717	0.714	—	—	—	—	—
	CNN-Multimodal (Hollenstein et al. 2021)	—	—	—	—	0.738	0.724	0.723	—	—	—	—	—
	Ours-EEG	<b>0.984</b>	<b>0.991</b>	<b>0.989</b>	<b>0.984</b>	<b>0.991</b>	<b>0.997</b>	<b>0.994</b>	<b>0.990</b>	<b>0.891</b>	<b>0.888</b>	<b>0.889</b>	<b>0.890</b>
	Ours-Text	<b>0.850</b>	<b>0.849</b>	<b>0.849</b>	<b>0.817</b>	<b>0.832</b>	<b>0.834</b>	<b>0.833</b>	<b>0.839</b>	<b>0.823</b>	<b>0.881</b>	<b>0.850</b>	<b>0.891</b>
	Ours-Multimodal	<b>0.989</b>	<b>0.997</b>	<b>0.993</b>	<b>0.993</b>	<b>0.986</b>	<b>0.977</b>	<b>0.981</b>	<b>0.994</b>	<b>0.966</b>	<b>0.975</b>	<b>0.970</b>	<b>0.978</b>
Relation Detection	MLP-EEG	0.450	0.455	0.452	0.450	0.463	0.471	0.467	0.463	0.435	0.438	0.436	0.430
	MLP-Text	0.191	0.214	0.192	0.254	0.249	0.286	0.266	0.258	0.228	0.231	0.229	0.230
	BiLSTM-EEG	0.552	0.570	0.556	0.549	0.584	0.591	0.587	0.585	0.564	0.541	0.552	0.551
	BiLSTM-Text	0.153	0.173	0.149	0.186	0.200	0.199	0.199	0.201	0.182	0.133	0.154	0.148
	Transformer-EEG	0.589	0.517	0.551	0.564	0.399	0.401	0.400	0.421	0.364	0.372	0.368	0.370
	Transformer-Text	0.428	0.487	0.444	0.420	0.488	0.491	0.489	0.487	0.301	0.299	0.300	0.300
	ResNet-EEG	0.514	0.571	0.590	0.558	0.499	0.501	0.500	0.500	0.503	0.519	0.511	0.504
	ResNet-Text	0.314	0.283	0.265	0.322	0.311	0.336	0.323	0.326	0.278	0.289	0.283	0.288
	CNN-Multimodal (Hollenstein et al. 2021)	—	—	—	—	0.647	0.664	0.650	—	—	—	—	—
	RNN-Multimodal (Hollenstein et al. 2021)	—	—	—	—	0.652	0.690	0.668	—	—	—	—	—
	Ours-EEG	<b>0.942</b>	<b>0.976</b>	<b>0.959</b>	<b>0.932</b>	<b>0.922</b>	<b>0.938</b>	<b>0.930</b>	<b>0.931</b>	<b>0.900</b>	<b>0.943</b>	<b>0.921</b>	<b>0.922</b>
	Ours-Text	<b>0.743</b>	<b>0.751</b>	<b>0.747</b>	<b>0.732</b>	<b>0.744</b>	<b>0.784</b>	<b>0.763</b>	<b>0.759</b>	<b>0.634</b>	<b>0.686</b>	<b>0.659</b>	<b>0.660</b>
	Ours-Multimodal	<b>0.979</b>	<b>0.987</b>	<b>0.979</b>	<b>0.982</b>	<b>0.977</b>	<b>0.980</b>	<b>0.978</b>	<b>0.984</b>	<b>0.969</b>	<b>0.965</b>	<b>0.967</b>	<b>0.969</b>

(31–39.75Hz), and middle-gamma (41–49.75Hz). We used Google Cloud’s Speech-to-Text API to transcribe the audio data into text.

**ZuCo Dataset** The ZuCo Dataset (Hollenstein et al. 2018, 2020) is a corpus of EEG signals and eye tracking data during natural reading. The tasks during natural reading can be separated into three categories: sentiment analysis, natural reading, and task specified reading. During sentiment analysis, the participant was presented with 400 positive, neutral, and negative labeled sentences from the Stanford Sentiment Treebank (Socher et al. 2013). The EEG data used in this study can be categorized into sentence-level and word-level features. The sentence-level features are the averaged word-level EEG features for the entire sentence duration. The word-level EEG features are for the first fixation duration (FFD) of a specific word, meaning when the participant’s eye met the word, the EEG signals were recorded. For both word and sentence-level features, 8 frequency bands were recorded at a sampling frequency of 500 Hz and denoted as the following: theta1 (4–6Hz), theta2 (6.5–8Hz), alpha1 (8.5–10Hz), alpha2 (10.5–13Hz), beta1 (13.5–18Hz), beta2 (18.5–30Hz) and gamma1 (30.5–40Hz) and gamma2 (40–49.5Hz).

## Experimental Settings

The hierarchical transformer encoders follow the standard skeleton from Vaswani et al. (2017), excluding its complexity. To avoid overfitting, we adopt the oversampling strategy for data augmentation (Hübschle-Schneider and Sanders 2019), which ensures a balanced distribution of classes included in each batch. The train/test/validation splitting is (80%, 10%, 10%) as in Hollenstein et al. (2021). The EEG features are extracted from the datasets in 8 frequency bands

and normalized with Z-score according to previous work (S. Yousif et al. 2020; Fdez et al. 2021; Du et al. 2022) over each frequency band. To preserve relatability, the word and sentence embeddings are also normalized with Z-scores. We use pre-trained language models to generate text features (Devlin et al. 2019), where all texts are tokenized and embedded using the BERT-uncased-base model. Each sentence has an average length of 20 tokens, so we instantiate a max length of 32 with padding. In the case of word-level, we use an average length of 4 tokens for each word and establish a max length of 10 with padding. The token vectors’ from the four last hidden layers of the pre-trained model are withdrawn and averaged to get a final sentence or word embedding. These embeddings are used during the sentence-level and word-level settings. For concat word-level, we simply concatenate the word embeddings for their respective sentence. All the experimental parameters are listed in the Appendix due to page limit.

## Baselines

The area of multimodal learning of EEG and language is not well explored, and to the best of our knowledge, only Hollenstein et al. (2021)’s approach was directly comparable to our study. However, to make a fair evaluation, we implemented the following state-of-the-art representative approaches as baselines for verification: MLP (Ruppert 2004), Bi-LSTM (Zhou et al. 2016), Transformer (Vaswani et al. 2017), and ResNet (He et al. 2016).

## Experimental Results and Discussions

In Table 2, we show the comparison results of different methods on the K-EmoCon dataset. From Table 2, we can see that our method outperforms the other baselines, and the



multimodal approach outperforms the unimodal approach, which also demonstrates the effectiveness of our method. In Table 1, we show the comparison results of the ZuCo dataset for Sentiment Analysis and Relation Detection, respectively. Our method outperforms all baselines, and the multimodal approach outperforms unimodal approaches, which further demonstrates the importance of exploring the inner alignment between EEG and language.

Table 2: Comparison with baselines on K-EmoCon dataset for Sentiment Analysis.

Model	Prec	Rec	F1	Acc
MLP-EEG	0.295	0.317	0.222	0.231
MLP-Text	0.263	0.272	0.182	0.180
BiLSTM-EEG	0.340	0.354	0.226	0.220
BiLSTM-Text	0.241	0.329	0.125	0.224
Transformer-EEG	0.399	0.411	0.405	0.484
Transformer-Text	0.454	0.492	0.472	0.443
ResNet-EEG	0.456	0.389	0.202	0.229
ResNet-Text	0.133	0.348	0.169	0.224
Ours-EEG	<b>0.591</b>	<b>0.516</b>	<b>0.551</b>	<b>0.591</b>
Ours-Text	<b>0.524</b>	<b>0.561</b>	<b>0.509</b>	<b>0.542</b>
Ours-Multimodal	<b>0.739</b>	<b>0.720</b>	<b>0.729</b>	<b>0.733</b>

## Ablation Study

To further investigate the performance of different mechanisms in the CAM module, we carried out ablation experiments on the Zuco dataset, and the results are shown in Table 3. The combination of CCA and WD performed better compared to using only one mechanism for sentiment analysis and relation detection in all model settings.

We also conducted experiments on word-level, sentence-level, and concat word-level inputs, and the results are also shown in Table 3. We observe that word-level EEG features paired with its respective word generally outperforms sentence-level and concat word-level in both tasks.

## Analysis

In order to interpret the performance improvement, we visualized the original feature distribution and the transformed feature distribution. As shown in Fig. 3, the transformed feature distribution makes better clusters than the original one. The alignment module reduces the randomness and sparsity, showing the effectiveness of discovering and encoding the relationship between EEG and language.

Furthermore, to understand the alignment between language and EEG, we visualize the alignment weights of word-level EEG-language alignment on the ZuCo dataset. Fig. 4 and Fig. 5 show examples of negative & positive sentence word-level alignment, respectively. The sentence-level alignment visualization are shown in Appendix.

From the word level alignment in Fig. 4 and Fig. 5, beta2 and gamma1 waves are most active. This is consistent with the literature, which showed that gamma waves are seen to be active in detecting emotions (Li and Lu 2009) and beta waves have been involved in higher order linguistic functions (e.g., discrimination of word categories) (Hollenstein et al. 2021). Hollenstein et al. (2021) found that beta and theta waves were most useful in terms of model performance in sentiment analysis.

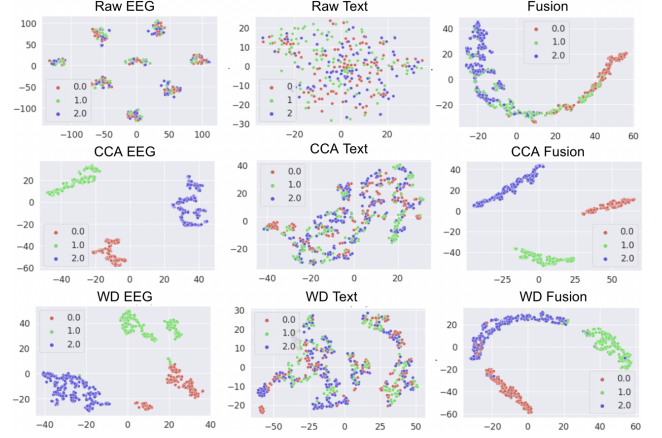


Figure 3: TSNE projection comparison of untransformed & transformed features of ZuCo dataset.

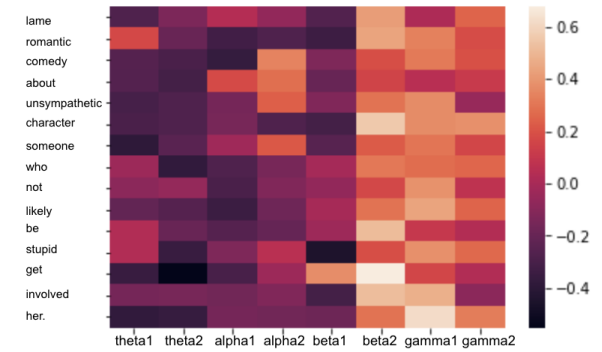


Figure 4: Negative word-level alignment from ZuCo dataset.

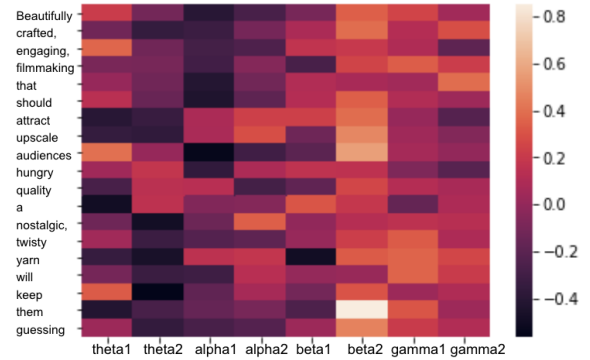


Figure 5: Positive word-level alignment from ZuCo dataset.

We performed an analysis of which EEG feature refined the model’s performance since different neurocognitive factors during language processing are associated with brain oscillations at miscellaneous frequencies. The beta and theta bands have positively contributed the most, which is due to the theta band power expected to rise with increased language processing activity and the band’s relation to semantic memory retrieval (Kosch et al. 2020; Hollenstein et al. 2021). The beta’s contribution can be best explained by the effect of emotional connotations of the text (Bastiaansen et al. 2005; Hollenstein et al. 2021).

Table 3: Ablation results on the components in the CAM module.

Dataset	Model	Sentence Level				Word Level				Concat Word Level			
		Prec	Rec	F1	Acc	Prec	Rec	F1	Acc	Prec	Rec	F1	Acc
ZuCo (SA)	Ours-CCA-Text	0.748	0.746	0.747	0.707	0.701	0.733	0.717	0.769	0.752	0.787	0.769	0.744
	Ours-CCA-EEG	0.984	0.991	0.989	0.984	0.988	0.991	0.989	0.985	<b>0.970</b>	0.975	0.972	0.971
	Ours-CCA-All	0.987	0.956	0.971	0.991	0.989	0.979	0.984	0.991	0.959	0.973	0.966	0.972
	Ours-WD-Text	0.618	0.604	0.611	0.624	0.753	0.747	0.750	0.770	0.740	0.731	0.735	0.733
	Ours-WD-EEG	0.965	0.930	0.942	0.948	0.982	<b>0.999</b>	0.990	0.991	0.888	0.882	0.885	0.867
	Ours-WD-All	0.910	0.862	0.885	0.981	0.985	<b>0.999</b>	0.992	0.994	0.918	0.922	<b>0.985</b>	0.917
	Ours-CCA+WD-Text	0.850	0.849	0.849	0.817	0.832	0.834	0.833	0.839	0.823	0.881	0.850	0.891
	Ours-CCA+WD-EEG	0.979	0.982	0.980	0.983	<b>0.991</b>	0.997	<b>0.994</b>	0.990	0.891	0.888	0.889	0.890
	Ours-CCA+WD-All	<b>0.989</b>	<b>0.997</b>	<b>0.993</b>	<b>0.993</b>	0.986	0.977	0.981	<b>0.994</b>	0.966	<b>0.975</b>	0.970	<b>0.978</b>
	Ours-CCA-Text	0.750	0.749	0.749	0.717	0.698	0.661	0.679	0.650	0.551	0.655	0.599	0.602
	Ours-CCA-EEG	0.851	0.926	0.874	0.863	0.780	0.781	0.780	0.782	0.744	0.801	0.771	0.750
	Ours-CCA-All	0.892	0.930	0.885	0.881	0.911	0.923	0.917	0.904	0.851	0.866	0.858	0.855
ZuCo (RD)	Ours-WD-Text	0.674	0.642	0.658	0.668	0.671	0.624	0.647	0.651	0.597	0.577	0.587	0.599
	Ours-WD-EEG	0.870	0.867	0.868	0.847	0.899	0.908	0.903	0.900	0.891	0.925	0.908	0.900
	Ours-WD-All	0.802	0.857	0.829	0.880	0.898	0.943	0.920	0.914	0.898	0.866	0.882	0.916
	Ours-CCA+WD-Text	0.743	0.751	0.747	0.732	0.744	0.784	0.763	0.759	0.634	0.686	0.659	0.660
	Ours-CCA+WD-EEG	0.942	0.976	0.959	0.932	0.922	0.938	0.930	0.931	0.900	0.943	0.921	0.922
	Ours-CCA+WD-All	<b>0.979</b>	<b>0.987</b>	<b>0.979</b>	<b>0.982</b>	<b>0.977</b>	<b>0.980</b>	<b>0.978</b>	<b>0.984</b>	<b>0.969</b>	<b>0.965</b>	<b>0.967</b>	<b>0.969</b>

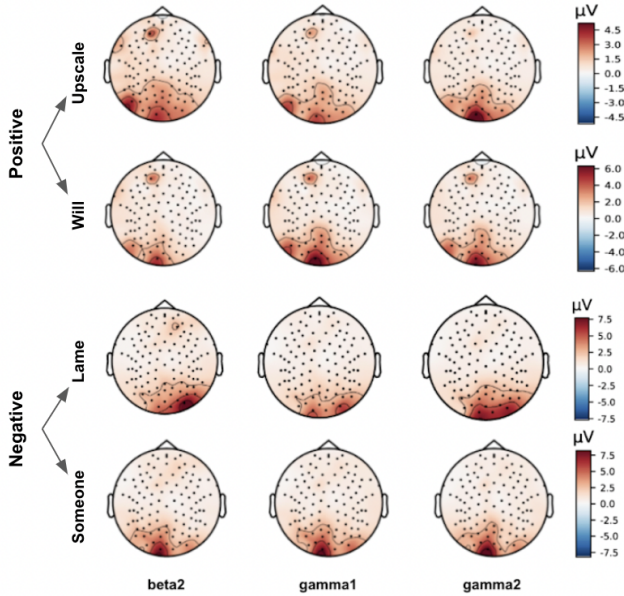


Figure 6: Most relevant positive and negative word brain topologies (beta1, gamma1, and gamma2).

In Fig. 6, we visualized the brain topologies with word-level EEG features for a pair of important and unimportant words from the positive and negative labeled sentences in the ZuCo dataset. We deemed a word important if the definition had a positive or negative connotation. 'Upscale' and 'lame' are the important positive and negative words, respectively, and 'will' and 'someone' are the unimportant positive and negative words, respectively. There are two areas in the brain that are heavily associated with language processing: Broca's area and Wernicke's area. Broca's area is assumed to be located in the left frontal lobe, and this region is concerned with the production of speech (Nasios, Dardiotis, and Messinis 2019). The left posterior superior temporal gyrus is typically assumed as Wernicke's area, and this locale is involved with the comprehension of speech (Nasios, Dardi-

otis, and Messinis 2019).

Similar to Fig. 4 and Fig. 5, we can observe the beta2, gamma1, and gamma2 frequency bands having the most powerful signals for all words. In Fig. 6, activity in Wernicke's area can be seen most visibly in the beta2, gamma1, and gamma2 bands for the words 'Upscale' and 'Will'. For the word 'Upscale,' we also saw activity around Broca's area for alpha1, alpha2, beta1, beta2, theta1, and theta2 bands. An interesting observation is that for the negative words, 'Lame' and 'Someone', we see very low activation in Broca's and Wernicke's areas. Instead, we see most of the activity in the occipital lobes and slightly over the inferior parietal lobes. The occipital lobes are noted as the visual processing area of the brain and are associated with memory formation, face recognition, distance and depth interpretation, and visuospatial perception (Rehman and Khalili 2019). The inferior parietal lobes are generally found to be key actors in visuospatial attention and semantic memory (Numssen, Bzdok, and Hartwigsen 2021).

## Conclusion

In this study, we explore the relationship between EEG and language. We propose MTAM, a Multimodal Transformer Alignment Model, to observe coordinated representations between the two modalities and employ the transformed representations for downstream applications. Our method achieved state-of-the-art performance on sentiment analysis and relation detection tasks on two datasets, ZuCo and K-EmoCon. Furthermore, we carried out a comprehensive study to analyze the connectivity and alignment between EEG and language. We observed that the transformed features show less randomness and sparsity. The word-level language-EEG alignment clearly demonstrated the importance of the explored connectivity. We also provided brain topologies as an intuitive understanding of the corresponding activity regions in the brain, which could build the neuropsychological basis for understanding the relationship between EEG and language through computational models.

## References

- Andrew, G.; Arora, R.; Bilmes, J.; and Livescu, K. 2013. Deep Canonical Correlation Analysis. 28.
- Bao, L.-Q.; Qiu, J.-L.; Tang, H.; Zheng, W.-L.; and Lu, B.-L. 2019. Investigating Sex Differences in Classification of Five Emotions from EEG and Eye Movement Signals. *2019 41st Annual International Conference of the IEEE Engineering in Medicine and Biology Society (EMBC)*, 6746–6749.
- Bashar, K. 2018. ECG and EEG Based Multimodal Biometrics for Human Identification.
- Bastiaansen, M. C. M.; van der Linden, M.; Ter Keurs, M.; Dijkstra, T.; and Hagoort, P. 2005. Theta responses are involved in lexical-semantic retrieval during language processing. *Journal of Cognitive Neuroscience*, 17: 530–541.
- Ben Said, A.; Mohamed, A.; Elfouly, T.; Harras, K.; and Wang, Z. J. 2017. Multimodal Deep Learning Approach for Joint EEG-EMG Data Compression and Classification.
- Bisk, Y.; Holtzman, A.; Thomason, J.; Andreas, J.; Bengio, Y.; Chai, J.; Lapata, M.; Lazaridou, A.; May, J.; Nisnevich, A.; Pinto, N.; and Turian, J. 2020. Experience Grounds Language.
- Brown, T. B.; Mann, B.; Ryder, N.; Subbiah, M.; Kaplan, J.; Dhariwal, P.; Neelakantan, A.; Shyam, P.; Sastry, G.; Askell, A.; Agarwal, S.; Herbert-Voss, A.; Krueger, G.; Henighan, T. J.; Child, R.; Ramesh, A.; Ziegler, D. M.; Wu, J.; Winter, C.; Hesse, C.; Chen, M.; Sigler, E.; Litwin, M.; Gray, S.; Chess, B.; Clark, J.; Berner, C.; McCandlish, S.; Radford, A.; Sutskever, I.; and Amodei, D. 2020. Language Models are Few-Shot Learners. *ArXiv*, abs/2005.14165.
- Chen, L.; Gan, Z.; Cheng, Y.; Li, L.; Carin, L.; and Liu, J. 2020. Graph Optimal Transport for Cross-Domain Alignment. *ArXiv*, abs/2006.14744.
- Choi, J.; Jung, E.; Suh, J.; and Rhee, W. 2021. Improving Bi-encoder Document Ranking Models with Two Rankers and Multi-teacher Distillation. *Proceedings of the 44th International ACM SIGIR Conference on Research and Development in Information Retrieval*, 2192–2196.
- Correia, J.; Formisano, E.; Valente, G.; Hausfeld, L.; Jansma, B.; and Bonte, M. 2013. Brain-Based Translation: fMRI Decoding of Spoken Words in Bilinguals Reveals Language-Independent Semantic Representations in Anterior Temporal Lobe. *Journal of Neuroscience*, 34: 332–338.
- Culotta, A.; McCallum, A.; and Betz, J. 2006. Integrating Probabilistic Extraction Models and Data Mining to Discover Relations and Patterns in Text. In *Proceedings of the Human Language Technology Conference of the NAACL, Main Conference*, 296–303. Association for Computational Linguistics.
- Demetci, P.; Santorella, R.; Sandstede, B.; Noble, W. S.; and Singh, R. 2020. Gromov-Wasserstein optimal transport to align single-cell multi-omics data. *bioRxiv*.
- Deng, L. 2016. Deep learning: from speech recognition to language and multimodal processing. *APSIPA Transactions on Signal and Information Processing*, 5.
- Deniz, F.; Tseng, C.; Wehbe, L.; and Gallant, J. L. 2021. Semantic representations during language comprehension are affected by context. *bioRxiv*.
- Devlin, J.; Chang, M.-W.; Lee, K.; and Toutanova, K. 2019. BERT: Pre-training of Deep Bidirectional Transformers for Language Understanding. *ArXiv*, abs/1810.04805.
- Du, Y.; Xu, Y.; Wang, X.; Liu, L.; and Ma, P. 2022. ETST: EEG Transformer for Person Identification.
- Elliott, D.; Kiela, D.; and Lazaridou, A. 2016. Multimodal Learning and Reasoning. In *ACL 2016*.
- Fdez, J.; Guttenberg, N.; Witkowski, O.; and Pasquali, A. 2021. Cross-Subject EEG-Based Emotion Recognition Through Neural Networks With Stratified Normalization. *Frontiers in Neuroscience*, 15.
- Foster, C.; Williams, C. C.; Krigolson, O. E.; and Fyshe, A. 2021. Using EEG to decode semantics during an artificial language learning task. *Brain and Behavior*, 11.
- Gauthier, J.; and Ivanova, A. A. 2018. Does the brain represent words? An evaluation of brain decoding studies of language understanding. *ArXiv*, abs/1806.00591.
- Gong, Y.; Ke, Q.; Isard, M.; and Lazebnik, S. 2013. A Multi-View Embedding Space for Modeling Internet Images, Tags, and Their Semantics. *International Journal of Computer Vision*, 106: 210–233.
- Hale, J.; Kuncoro, A.; Hall, K. B.; Dyer, C.; and Brennan, J. 2019. Text Genre and Training Data Size in Human-like Parsing. In *EMNLP*.
- He, K.; Zhang, X.; Ren, S.; and Sun, J. 2016. Deep Residual Learning for Image Recognition. *2016 IEEE Conference on Computer Vision and Pattern Recognition (CVPR)*, 770–778.
- Hollenstein, N.; Barrett, M.; and Beinborn, L. 2020. Towards Best Practices for Leveraging Human Language Processing Signals for Natural Language Processing. In *LINCR*.
- Hollenstein, N.; Barrett, M.; Troendle, M.; Bigiolli, F.; Langer, N.; and Zhang, C. 2019. Advancing NLP with Cognitive Language Processing Signals. *ArXiv*, abs/1904.02682.
- Hollenstein, N.; Renggli, C.; Glaus, B. J.; Barrett, M.; Troendle, M.; Langer, N.; and Zhang, C. 2021. Decoding EEG Brain Activity for Multi-Modal Natural Language Processing. *Frontiers in Human Neuroscience*, 15.
- Hollenstein, N.; Rotsztein, J.; Troendle, M.; Pedroni, A.; Zhang, C.; and Langer, N. 2018. ZuCo, a simultaneous EEG and eye-tracking resource for natural sentence reading. *Scientific Data*, 5.
- Hollenstein, N.; Troendle, M.; Zhang, C.; and Langer, N. 2020. ZuCo 2.0: A Dataset of Physiological Recordings During Natural Reading and Annotation. *arXiv:1912.00903 [cs]*.
- Huang, S.-C.; Pareek, A.; Zamanian, R.; Banerjee, I.; and Lungren, M. P. 2020. Multimodal fusion with deep neural networks for leveraging CT imaging and electronic health record: a case-study in pulmonary embolism detection. *Scientific Reports*, 10: 22147.
- Huang, Y.; Du, C.; Xue, Z.; Chen, X.; Zhao, H.; and Huang, L. 2021. What Makes Multimodal Learning Better than Single (Provably). In *NeurIPS*.



- Hübschle-Schneider, L.; and Sanders, P. 2019. Parallel Weighted Random Sampling. *ACM Transactions on Mathematical Software (TOMS)*.
- Kiros, R.; Salakhutdinov, R.; and Zemel, R. S. 2014. Multimodal Neural Language Models. In *ICML*.
- Koelstra, S.; Muhl, C.; Soleymani, M.; Lee, J.-S.; Yazdani, A.; Ebrahimi, T.; Pun, T.; Nijholt, A.; and Patras, I. 2012. DEAP: A Database for Emotion Analysis ;Using Physiological Signals. *IEEE Transactions on Affective Computing*, 3: 18–31.
- Kosch, T.; Schmidt, A.; Thanheiser, S.; and Chuang, L. L. 2020. One does not Simply RSVP: Mental Workload to Select Speed Reading Parameters using Electroencephalography. *Proceedings of the 2020 CHI Conference on Human Factors in Computing Systems*.
- Lee, J.; Dabagia, M.; Dyer, E. L.; and Rozell, C. J. 2019. Hierarchical Optimal Transport for Multimodal Distribution Alignment. *ArXiv*, abs/1906.11768.
- Lewis, M.; Liu, Y.; Goyal, N.; Ghazvininejad, M.; Mohamed, A.; Levy, O.; Stoyanov, V.; and Zettlemoyer, L. 2020. BART: Denoising Sequence-to-Sequence Pre-training for Natural Language Generation, Translation, and Comprehension. In *ACL*.
- Li, M.; and Lu, B.-L. 2009. Emotion classification based on gamma-band EEG. *Annual International Conference of the IEEE Engineering in Medicine and Biology Society. IEEE Engineering in Medicine and Biology Society. Annual International Conference*, 2009: 1323–1326.
- Linzen, T. 2020. How Can We Accelerate Progress Towards Human-like Linguistic Generalization? In *ACL*.
- Liu, W.; Qiu, J.-L.; Zheng, W.-L.; and Lu, B.-L. 2019a. Multimodal Emotion Recognition Using Deep Canonical Correlation Analysis. *ArXiv*, abs/1908.05349.
- Liu, W.; Qiu, J.-L.; Zheng, W.-L.; and Lu, B.-L. 2022. Comparing Recognition Performance and Robustness of Multimodal Deep Learning Models for Multimodal Emotion Recognition. *IEEE Transactions on Cognitive and Developmental Systems*, 14: 715–729.
- Liu, Y.; Ott, M.; Goyal, N.; Du, J.; Joshi, M.; Chen, D.; Levy, O.; Lewis, M.; Zettlemoyer, L.; and Stoyanov, V. 2019b. RoBERTa: A Robustly Optimized BERT Pretraining Approach. *ArXiv*, abs/1907.11692.
- McGurk, H.; and MacDonald, J. 1976. Hearing lips and seeing voices. *Nature*, 264: 746–748.
- Morency, L.-P.; and Baltrusaitis, T. 2017. Multimodal Machine Learning: Integrating Language, Vision and Speech. In *ACL*.
- Murphy, A.; Bohnet, B.; McDonald, R. T.; and Noppeney, U. 2022. Decoding Part-of-Speech from Human EEG Signals. In *ACL*.
- Murphy, B.; Wehbe, L.; and Fyshe, A. 2018. Decoding Language from the Brain.
- Nasios, G.; Dardiotis, E.; and Messinis, L. 2019. From Broca and Wernicke to the Neuromodulation Era: Insights of Brain Language Networks for Neurorehabilitation. *Behavioural Neurology*, 2019.
- Numssen, O.; Bzdok, D.; and Hartwigsen, G. 2021. Functional specialization within the inferior parietal lobes across cognitive domains. *eLife*, 10.
- Ortega, P.; and Faisal, A. A. 2021. Deep learning multimodal fNIRS and EEG signals for bimanual grip force decoding. *Journal of Neural Engineering*, 18.
- Park, C. Y.; Cha, N.; Kang, S.; Kim, A.; Khandoker, A. H.; Hadjileontiadis, L.; Oh, A.; Jeong, Y.; and Lee, U. 2020. K-EmoCon, a multimodal sensor dataset for continuous emotion recognition in naturalistic conversations. *Scientific Data*, 7.
- Qiu, J.; Zhu, J.; Xu, M.; Dernoncourt, F.; Bui, T.; Wang, Z.; Li, B.; Zhao, D.; and Jin, H. 2022. MHMS: Multimodal Hierarchical Multimedia Summarization. *ArXiv*, abs/2204.03734.
- Qiu, J.-L.; Liu, W.; and Lu, B.-L. 2018. Multi-view Emotion Recognition Using Deep Canonical Correlation Analysis. In *ICONIP*.
- Reddy, A. J.; and Wehbe, L. 2021. Can fMRI reveal the representation of syntactic structure in the brain? *bioRxiv*.
- Rehman, A.; and Khalili, Y. A. 2019. Neuroanatomy, Occipital Lobe.
- Ruppert, D. 2004. The Elements of Statistical Learning: Data Mining, Inference, and Prediction. *Journal of the American Statistical Association*, 99: 567 – 567.
- S. Yousif, E.; Shawkat Abdulbaqi, A.; Zaily Hameed, A.; and Al-din M. N, S. 2020. Electroencephalogram Signals Classification Based on Feature Normalization. *IOP Conference Series: Materials Science and Engineering*, 928: 032028.
- Saeidi, M.; Karwowski, W.; Farahani, F. V.; Fiok, K.; Taiar, R.; Hancock, P. A.; and Al-Juaid, A. 2021. Neural Decoding of EEG Signals with Machine Learning: A Systematic Review. *Brain Sciences*, 11.
- Schwartz, D.; Toneva, M.; and Wehbe, L. 2019. Inducing brain-relevant bias in natural language processing models. In *NeurIPS*.
- Socher, R.; Perelygin, A.; Wu, J.; Chuang, J.; Manning, C. D.; Ng, A.; and Potts, C. 2013. Recursive Deep Models for Semantic Compositionality Over a Sentiment Treebank. In *Proceedings of the 2013 Conference on Empirical Methods in Natural Language Processing*, 1631–1642.
- Stemmer, B.; and Connolly, J. 2012. The EEG/ERP technologies in linguistic research.
- Tiippana, K. 2014. What is the McGurk effect? *Frontiers in Psychology*, 5.
- Toneva, M.; Mitchell, T.; and Wehbe, L. 2020. Combining computational controls with natural text reveals new aspects of meaning composition. *bioRxiv*.
- Toneva, M.; and Wehbe, L. 2019. Interpreting and improving natural-language processing (in machines) with natural language-processing (in the brain). *ArXiv*, abs/1905.11833.
- Vaswani, A.; Shazeer, N.; Parmar, N.; Uszkoreit, J.; Jones, L.; Gomez, A.; Kaiser, Ł.; and Polosukhin, I. 2017. Attention Is All You Need.

Wang, Z.; and Ji, H. 2021. Open Vocabulary Electroencephalography-To-Text Decoding and Zero-shot Sentiment Classification. *ArXiv*, abs/2112.02690.

Wehbe, L.; Blank, I. A.; Shain, C.; Futrell, R.; Levy, R. P.; von der Malsburg, T.; Smith, N. J.; Gibson, E.; and Fedorenko, E. 2020. Incremental language comprehension difficulty predicts activity in the language network but not the multiple demand network. *bioRxiv*.

Wehbe, L.; Vaswani, A.; Knight, K.; and Mitchell, T. 2014. Aligning context-based statistical models of language with brain activity during reading.

Williams, J.; and Wehbe, L. 2021. Behavior measures are predicted by how information is encoded in an individual's brain. *ArXiv*, abs/2112.06048.

Yang, Z.; Dai, Z.; Yang, Y.; Carbonell, J. G.; Salakhutdinov, R.; and Le, Q. V. 2019. XLNet: Generalized Autoregressive Pretraining for Language Understanding. In *NeurIPS*.

Yang, Z.; Fang, Y.; Zhu, C.; Pryzant, R.; Chen, D.; Shi, Y.; Xu, Y.; Qian, Y.; Gao, M.; Chen, Y.-L.; Lu, L.; Xie, Y.; Gmyr, R.; Codella, N.; Kanda, N.; Xiao, B.; Yuan, L.; Yoshioka, T.; Zeng, M.; and Huang, X. 2022. i-Code: An Integrative and Composable Multimodal Learning Framework. *arXiv:2205.01818*.

Yuan, S.; Bai, K.; Chen, L.; Zhang, Y.; Tao, C.; Li, C.; Wang, G.; Henao, R.; and Carin, L. 2020. Advancing weakly supervised cross-domain alignment with optimal transport. *ArXiv*, abs/2008.06597.

Yuhas, B.; Goldstein, M.; and Sejnowski, T. 1989. Integration of acoustic and visual speech signals using neural networks. *IEEE Communications Magazine*, 27: 65–71.

Zheng, W.-L.; and Lu, B.-L. 2015. Investigating Critical Frequency Bands and Channels for EEG-Based Emotion Recognition with Deep Neural Networks. *IEEE Transactions on Autonomous Mental Development*, 7: 162–175.

Zhou, P.; Shi, W.; Tian, J.; Qi, Z.; Li, B.; Hao, H.; and Xu, B. 2016. Attention-Based Bidirectional Long Short-Term Memory Networks for Relation Classification. *Proceedings of the 54th Annual Meeting of the Association for Computational Linguistics*.

Zhu, J.; Qiu, J.; Yang, Z.; Weber, D.; Rosenberg, M. A.; Liu, E.; Li, B.; and Zhao, D. 2022. GeoECG: Data Augmentation via Wasserstein Geodesic Perturbation for Robust Electrocardiogram Prediction. In *MLHC*.